since 1961

Baltica

BALTICA Volume 28 Number 2 December 2015: 65–80
doi: 10.5200/baltica.2015.28.07

Vertical ground movements in the Polish and Lithuanian Baltic coastal area as measured by satellite interferometry

Marek Graniczny, Jolanta Čyžienė, Freek van Leijen, Vytautas Minkevičius, Vidas Mikulėnas, Jonas Satkūnas, Maria Przyłucka, Zbigniew Kowalski, Szymon Uścinowicz, Wojciech Jegliński, Ramon Hanssen

Graniczny, M., Čyžienė, J., van Leijen, F., Minkevičius, V., Mikulėnas, V., Satkūnas, J., Przyłucka, M., Kowalski, Z., Uścinowicz, Sz., Jegliński, W., Hanssen, R., 2015. Vertical ground movements in the Polish and Lithuanian Baltic coastal area as measured by satellite interferometry. *Baltica, 28 (2), 65–80.* Vilnius. ISSN 0067-3064. doi: 10.5200/baltica.2015.28.07

Manuscript submitted 29 June 2015, revised 16 November 2015 / Accepted 26 November 2015 / Published online 10 December 2015
© Baltica 2015

Abstract The article contains results obtained from realization of the Polish and Lithuanian Baltic case study within the EU – FP 7 SubCoast project, which one of the primary aims was analysis of vertical ground movements, potentially causing geohazards in the coastal areas. To reach this goal Interferometric Synthetic Aperture Radar (InSAR) data were obtained. For the Polish and Lithuanian Baltic coast ERS archive radar data were processed in order to provide Permanent Scatterer (PSInSAR, PSI) results that were then used to create the new innovative product – Dynamic DEM (DDEM). The deformation model defined by the SubCoast project normally needs to be created by merging InSAR, satellite navigation (GNSS), optical leveling and/or gravimetry measurements. Elaboration of DDEM enables more effective comparison between PS and tectonic features. Comparison of PS time series with groundwater changes shows a direct correlation, confirming impact of groundwater on subsidence or uplift of the ground surface. The results of the geological interpretation demonstrated that the examples of movements detected by PSI include subsidence linked to deformation of engineering constructions, compaction of organic or weak soils, and eolian accumulation or deflation processes of the sand dunes. For the Polish and Lithuanian coasts most of the area proved to be stable, nevertheless some local deviations up to –15 mm per year of movement were found.

Keywords *·• Baltic coastal area·• satellite interferometry·• ground subsidence·• Dynamic-DEM*

✉ *Marek Graniczny (marek.graniczny@pgi.gov.pl), Maria Przyłucka (maria.przylucka@pgi.gov.pl), Zbigniew Kowalski (zbigniew.kowalski@pgi.gov.pl), Polish Geological Institute – National Research Institute, 4 Rakowiecka Street, 00975 Warsaw, Poland; Szymon Uścinowicz (szymon.uscinowicz@pgi.gov.pl), Wojciech Jegliński (wojciech.jeglinski@pgi.gov.pl), Polish Geological Institute – National Research Institute, Marine Geology Branch, Gdańsk, 5 Kościerska Street, 80328 Gdańsk, Poland; Jolanta Čyžienė (jolanta.cyziene@lgt.lt), Vytautas Minkevičius (vytautas.minkevicius@lgt.lt), Vidas Mikulėnas (vidas@lgt.lt), Jonas Satkūnas (jonas.satkunas@lgt.lt), Lithuanian Geological Survey, S. Konarskio str. 35, 03123 Vilnius, Lithuania; Freek van Leijen (F.J.vanLeijen@tudelft.nl), Ramon Hanssen (R.F.Hanssen@tudelft.nl), Delft University of Technology, Department of Geoscience and Remote Sensing, Stevinweg 1, 2628 CN Delft/PO box 5048, 2600 GA Delft, The Netherlands*

INTRODUCTION

Coastal lowland areas are widely recognized as highly vulnerable to the impacts of climate change, particularly sea-level rise and changes in runoff, as well as being subject to stresses imposed by human modification of catchment and delta plain land use. Utilization of the coast increased dramatically during the 20th century, a trend that seems certain to continue through the 21st century (Uścinowicz *et al*. 2004).

Rates of relative sea-level rise can significantly exceed the global average in many densely populat-

ed coastal lowland areas due to subsidence. Natural subsidence due to compaction of sediment under its weight is enhanced by sub-surface fluid withdrawals and drainage. This increases the potential for inundation, coastal erosion, habitat disruption and salt water intrusion, especially for the most populated cities of these coastal lowland areas. Typically, rates of subsidence vary over various spatial scales and depend strongly on local geological conditions and human activity.

Therefore, both from a viewpoint of imminent adverse effects from climate change in coastal lowland areas as Polish and Lithuanian Baltic Sea coasts. From the perspective of a sustainable management of infrastructural assets in these areas, there is a need of:

- Adequate data and information to assess spatial variations in subsidence in coastal lowland areas in relation to the sea level rise and its impact on flood risk.
- Adequate data and information to assess geographical and temporal variations in subsidence and its impact on the geological, ecological and hydrological systems in coastal lowland areas in order to anticipate necessary adaptive measures.
- Monitoring of the rate of settlement and movement of water defence structures and engineered constructions in order to detect any significant weaknesses in these structures in time.

GEOLOGICAL SETTING

The Polish Area of Interest (AoI) is located in the north-eastern part of Kaszuby Lakeland and the western part of the Vistula Delta plain, together with its coastal areas. The area covers in total 5000 km^2 (Fig. 1a). The area has a complex geologic structure. Precambrian crystalline bedrock occurs at the depth of ca. 4.5 km in the south-west to ca. 3.25 km in the north of the AoI. Along the Gulf of Gdansk coast crystalline bedrock occur at the depth of 3.25 km on NW and SW parts up to 3.75 km in the middle part, between Gdańsk and Gdynia (Pokorski, Modliński 2007)

The crystaline bedrock is covered by sedimentary rocks of the Uppermost Proterozoic-Devonian, Permian-Mesozoic and Cenozoic complexes. The top of the pre-Quaternary deposits is formed mainly by Neogene (Miocene) sand and silt. Oligocene and Eocene deposits occur locally in erosional depression in Kaszuby Lakeland. Long-lasting denudation processes at the end of the Neogene and the beginning of the Pleistocene, as well as glacial erosion during the earliest Pleistocene glaciation, are responsible for the origin of strongly sculptured top of pre-Quaternary deposits. The deepest tunnel valleys reach ca. 300 m below sea level (b.s.l.). The top of Cretaceous occur at a depths ca. 100 m b.s.l. in the area east and south-east of Gdansk in the Vistula Delta plain whereas the top of the Miocene reach locally to ca. 20–30 m above sea level (asl) in cliffs south and north of Gdynia and between Władysławowo and Jastrzębia Góra (Pikies 2000).

Pleistocene deposits are mainly of glacial and glaciofluvial origin. Their build strongly diversified terrain surface in Kaszuby Lakeland and the western and northern part of the coast whereas in Vistula Delta consist Holocene deposits. In the coastal zone of the Vistula Delta at the top of the Pleistocene occur mainly marine Eemian sands. The thickness of the Pleistocene ranges in general from a dozen to c. 250 meters in the Kaszuby Lakeland and ca. 60–40 m in the Vistula Delta. Holocene deposits in Kaszuby Lakeland occur locally in peatlands and in the valleys of rivers and lakes, having a thickness up to a few meters. The Holocene cover is much more uniform in the area of the Vistula Delta where deltaic sands, muds and locally peat reach totally up to 30 m (Mojski 1988).

The coast in the AoI east of Gdansk is of a barrier type with wide beaches and large dunes systems. North of Sopot occur sections of cliffs built by Pleistocene tills and sands and locally by Miocene deposits separated by short stretches of low alluvial coast with a narrow beaches developed in front of ice marginal valleys. There are two large cities, Gdansk and Gdynia, and several smaller cities located on the coast, inhabited by more than 1 mil. people.

The Lithuanian Area of Interest embraces the Lithuanian coastline of the Baltic Sea that is of 90.6 km long. Litho- and morphodynamic processes play an important role in the shore formation mechanism. On land they are determined mainly by aeolian processes and in the sea and on the beach by hydrodynamic ones (Fig. 1b).

A large part of the Baltic Sea coastal area in Lithuania is low-lying and therefore vulnerable to the predicted increasing in flooding, inundation and erosion which is expected as a result of thermal expansion of seawater and a melting of the ice caps as a consequence of climate change. Built-up settlements and coastal frontages are particularly susceptible to storm surges. Most damage to coasts is caused by extremes of sea levels during storm surges. In the South East Baltic waters, onshore waves are among the strongest in the entire Baltic Sea and hence a crucial issue in the assessment of safety levels of protective structures. Erosion and accretion are naturally occurring phenomena in the Lithuanian Baltic coast area which can often exist without human disturbance in a dynamic equilibrium. However, increasing human activity at

Fig. 1. Geographical localization of the Polish (a) and Lithuanian (b) Areas of Interest (red line, area analysed is onshore). Background source: Google Earth TM; compiled by M. Przyłucka and V. Minkevičius, 2015

the coast has accelerated erosion processes in many areas while causing accretion and sand shoaling in others.

The deposits that are found on the Lithuanian coastal area are formed during the Quaternary. There are two geologically and geomorphologically different sectors of the Lithuanian coastal area: the mainland sector (to the north from Klaipėda) and the Curonian Spit (Kuršių Nerija) (Bitinas *et al*. 2005). The mainland sector is geologically diverse. While sandy sediments that had formed mainly in the Littorina and Post-Littorina seas and their lagoons prevail in the northern part (Šventoji, Palanga), the southern part one (Nemirseta, Giruliai) is characterized by glacial (moraine) deposits formed during the Late Nemunas (LateWeichselian) and Medininkai (Saalian) glaciations (Bitinas *et al*. 1999), in most cases occurring in the abraded cliffs. A natural eolian beach dune occurs along the entire mainland coast. Its parameters vary from a height of 4–6 m and a width of 50–60 m at Būtingė or Melnragė to a height of 9–10 m and a width of 100–130 m to the south of Šventoji. Locally, the beach dune has been fully destroyed by abrasion caused by waves as well as by deflation. Processes of suffosion in the beach dune (developed on the 2–3 m high cliff composed of moraine) were observed close to Nemirseta. While in the northern part of the mainland, a Post-Litorina marine lagoon plain occurs behind a beach dune, glacial landforms formed during the Late Nemunas (Late Weichselian) glaciation may be traced to the south of Palanga (Bitinas *et al*. 2005).

The upper part of the Quaternary succession in the shore of the Curonian Spit is composed of deposits that had formed in the basins of various stages of the Baltic Sea development – starting from the Baltic Ice Lake and ending with recent marine sediments (Bitinas *et al*. 2001a, b). In the Curonian Spit, there is a man-made protective beach dune belt, whose formation started about 200 years ago, stretching along the entire length of the spit. Its height varies from 7–8 m to 15 m; the width mostly ranges from 50–60 m to 90–100 m. It should be noted that around Pervalka the beach dune widens to 150 m, acquiring a two-humped shape. Throughout the spit coast, a blown sand plain overgrown with plants occurs behind the protective beach dune. Apart from eolian sedimentation, intensive blowout processes as a result of which ravines, pits, moulds and so on have been formed characterize the beach dune.

MATERIAL AND METHODS

Space-borne differential synthetic aperture radar interferometry (DInSAR), and Persistent Scatterer Interferometry (PSInSAR or PSI; Ferretti *et al*. 2001, Bernardino *et al*. 2002), offer a unique possibility for wide-area, regular monitoring of ground surface displacements. Furthermore, under suitable conditions it should be possible to detect precursory deformations associated with the initiation of ground instability, as an essential element of early warning and hazard mitigation (Colesanti, Wasowski 2006; Ferretti *et al*. 2006). Satellite PSI data, however, have to be interpreted well. The Permanent Scatterers (PS) originate from objects on the surface, whose actual or apparent displacements may arise from a variety of causes (e.g. slope movements, fill settlement, subsurface civil engineering, mining and fluid extraction, differential movements between cut and fill parts of a building site, structure deterioration, expansion/shrinkage of soils (Colesanti *et al*. 2003; Bovenga *et al*. 2006; Culshaw 2009, Graniczny 2009; Hay-Man *et al*. 2009; Tomas *et al*. 2014; Del Ventisette *et al*. 2013)).

Satellite differential synthetic aperture radar interferometry (DInSAR), as introduced in early 1990, was used for detecting and monitoring ground surface deformations arising from regional scale processes e.g. seismic, volcanic, tectonic (Gabriel *et al*. 1989; Massonnet, Feigl 1998). The technique, however, was not effective for site-specific evaluations, because of

coarse resolution, coherence loss (a typical problem for vegetated areas) and atmospheric artefacts (e.g. Wasowski *et al*. 2002; Colesanti, Wasowski 2006).

The basic principles of PSInSAR were summarised by Colesanti and Wasowski (2006) as follows. The PS density varies from 0 to 500 points per square km depending on the land cover and the threshold set by phase stability to identify a point. High density of points allows to achieve 1 to 3 mm sensitivity in displacement measure. Dense PS grid is also essential for removing the atmospheric phase term. The PS analysis depends also on the number of SAR images (not less than 15-20). As a result of the processing the network of PS points with full displacement in Line-of-Sight (LOS) time series is acquired. The measurements are relative to the one master SAR image (in time) and to the one reference PS point (in space).

The effectiveness of PSI in monitoring ground deformations was confirmed by numerous examples of practical applications in different regions (e.g. Ferretti *et al*. 2006; *www.terrafirma.eu.com*).

PS data can assist in:

- Identification and delimitation of areas affected by slow deformations.
- Estimation of surface velocity and acceleration fields with millimetric precision.
- Identification of the source of ground instability by analysing *in situ* and multi-temporal remotely sensed data.

Terrestrial data were required both to realize their synergy with the space-based Earth Observation (EO) data and as a separate way of measuring the ground motion, for independent validation of the PSInSAR results. The former takes advantage of the fact that terrestrial networks measure ground motion at high resolution. PSInSAR provides the wide-area coverage, with hundreds of thousands of points. The terrestrial networks used include two GPS permanent stations, networks of piezometers, and measurements of sea-level by four tide-gauges. In addition, GIS data were used to integrate the observed ground motion, i.e., geological maps, hydrogeological maps, digital elevation models (DEM), lineaments, and geophysical data.

Full use of Persistant Scatterer-InSAR (PSInSAR) to map and monitor subsidence on a regional scale was applied in the project. The archived data from the ERS-1 and 2 (SAR-sensor) were acquired, processed and interpreted. For the Polish case study 60 SAR images were available on the track that covers the entire area of interest. 4 SAR scenes were discarded during processing due to poor quality, leaving a total of 56 SAR scenes in the final result. A total of 78093 PS points are detected in the data stack that spans the period 04/05/1992 to 07/12/2000. The vast majority of these points (80%) show a stable behaviour over this period.

For the Lithuanian case study 66 SAR images were available on the tracks which cover the entire area of interest. 6 SAR scenes were discarded during processing due to poor quality, leaving a total of 60 SAR scenes in the final result, spanning the 17/05/1992 to 15/11/2000 period. A total of 26 785 PS points are detected, with the vast majority of these points (87%) showing a stable motion over this period.

METHODOLOGY OF DYNAMIC-DEM CREATION

The Dynamic DEM (DDEM) concept defined within the SubCoast project *(http://www.subcoast.eu/)* aims to combine all available ground motion information, e.g., obtained by InSAR, satellite navigation (GNSS), optical leveling and/or gravimetry measurements, with a DEM. In case of Polish test site only InSAR measurement and two GNSS stations were available, therefore a simplified approach was applied. In the Lithuanian case one GPS station was used. The following steps were applied to create the Dynamic DEM, assuming a first-order linear behaviour, and accompanying quality description:

1. Estimate a trend for the GNSS stations, including accuracy.
2. Transform the GNSS station coordinates from WGS84 to a projected reference system, either using a national or European map projection, i.e. Transverse Mercator (ETRS89-TMzn).
3. Transform the PS coordinates from WGS84 to the planned reference system, either using a national or European map projection, i.e. Transverse Mercator (ETRS89-TMzn).
4. Predict the PS velocity at the GNSS station locations and determine the offset between the GPS and PS datasets.
5. Adapt the PS velocities and PS time series to the GNSS datum.
6. Remove outliers from the PS dataset.
7. Create a quadtree grid based on the PS grid (velocities + time series).
8. Create an equidistant grid based on the quadtree grid (velocities + time series).

Firstly, PSI velocity values were projected from the satellite Line-of-Sight (LOS) to the vertical direction in order to create a model of vertical ground movements in the area. The projection was done using (1):

$$\mathrm{Vel}^{\mathrm{VERT}} = \frac{\mathrm{Vel}^{\mathrm{LOS}}}{\cos\theta} \qquad (1),$$

were $\mathrm{Vel}^{\mathrm{VERT}}$ is velocity projected to vertical direction, $\mathrm{Vel}^{\mathrm{LOS}}$ is original velocity along the Light-of-Sight and θ is the incidence angle for the satellite, which is 23° in case of the ERS satellite.

To connect the PSI data to the datum set by the GNSS observations, a PSI deformation value should

be predicted at the location of the GNSS stations, to enable the estimation of a possible offset between the datums. In general it is very difficult to create a generic approach, since every location is different and complex deformation phenomena may occur. However, since the number of GNSS stations is always limited, a dedicated assessment of each station is possible. To connect the PSI measurements to a GNSS reference (based on the deformation rates), the following approaches are possible, in order of preference:

1. Connection based on PS in the same building. Since the GNSS antenna is typically fixed to a building or other structure, the GNSS measurements reflect both the stability of the particular building and the deformation of the (sub-)surface. For this reason connection to PS originating from the same building is recommended. However, sufficient PS should be available to detect outliers. Therefore, a minimum of 3 PS is required. The estimated height of PS points should be used to check whether the PS indeed originates from the building and not from the surface level.

The procedure is:

1. To calculate the mean and standard deviation of the PS velocities, possibly weighted based on a quality indicator such as standard deviation or coherence.
2. If (std > 0.5 mm/y), remove the biggest outlier with respect to the mean, and repeat. If number of PS becomes smaller than 3, this approach does not work, and apply option two instead.

2. In case the building does not contain (sufficient) PS, or not sufficient PS pass the outlier test of approach 1, use the surrounding area.

The procedure is:

1. Select the 25 nearest PS.
2. Calculate the mean, weighted mean, mean by inverse distance weighting, or Kriging, and the accompanying standard deviation.
3. Remove the PS outside the mean +/- Sigma range.
4. If the number of PS >= 15, re-calculate the mean and the standard deviation. If the standard deviation<0.5 mm/y, accept the PS. If reject, or the number of PS <15, select the next nearest points until again 25 PS are chosen, etc. If the standard deviation of the new iteration is worse than previous, take the previous solution as the final result.
5. Continue this approach until a maximum distance from the GNSS station is reached, e.g., 500 m. In this case, less than 15 points are used to estimate the reference offset.

To describe the quality of the quadtree blocks, the standard deviation of the PS velocity rates within a block are used. This standard deviation, σ_{obs}, is assumed to contain both the measurement noise, σ_n and the idealization precision or *signal noise*, σ_s, that is, the measure to describe how well the block value actually describes the signal. Hence,

$$\sigma_{obs} = \sigma_n + \sigma_s. \quad (2)$$

Based on the quadtree blocks a deformation model on a regular 100x100 m grid is created.

A visual inspection of the situation is still required. For example, when a firm deforming rail track with many PS is contained in the area, this may strongly influence the final result. In this case these PS should be excluded from the procedure a-priori.

RESULTS AND INTERPRETATION – POLISH CASE STUDY

Persistent Scatterer general results

The general results of the Persistent Scatterer processing for the Polish test site are presented on Fig. 2. A total of 78093 PS points are detected measuring velocities between – 4,08 and +25,85 mm/yr with a mean of –0,61 and a standard deviation of 1,29 mm/yr. It should be noted that 90% of all points (70520) have velocity rates between –2 and +2 mm per year. Therefore, in general the study area should be considered as stable. However, there are a few small areas where multiple PS exceed the stable values. In particular the area of the Gdynia-Gdansk agglomeration is characterized by values of about plus five millimeters per year, which may be related to groundwater level changes. Other observed anomalies are associated with small subsidence, probably related with local soil conditions.

Examples of local anomalies in the movement

The detection of numerous moving PS in the "LOTOS" Gdansk refinery site (Fig. 3A) is an interesting result of the PSI analysis. This site includes PS with very high average velocities (up to –10 mm/year). Specifically, both moving and non-moving PS are present in the refinery area. This, together with the geomorphological setting of the site (along the old natural canal within the Vistula river delta) and the presence of mud-rich alluvial deposits, locally containing organic material (peat), strongly suggest that the observed movements are caused by differential settlements induced by infrastructure loading of compressible sediments. It is of interest to note that the refinery was built in the seventies. The presence of such long-term settlements is perhaps not surprising considering the thickness (20–30 m) of the compressible materials and the heavy infrastructure characteristics.

An interesting phenomenon related to subsidence of up to –7 mm/year of the railway section near village

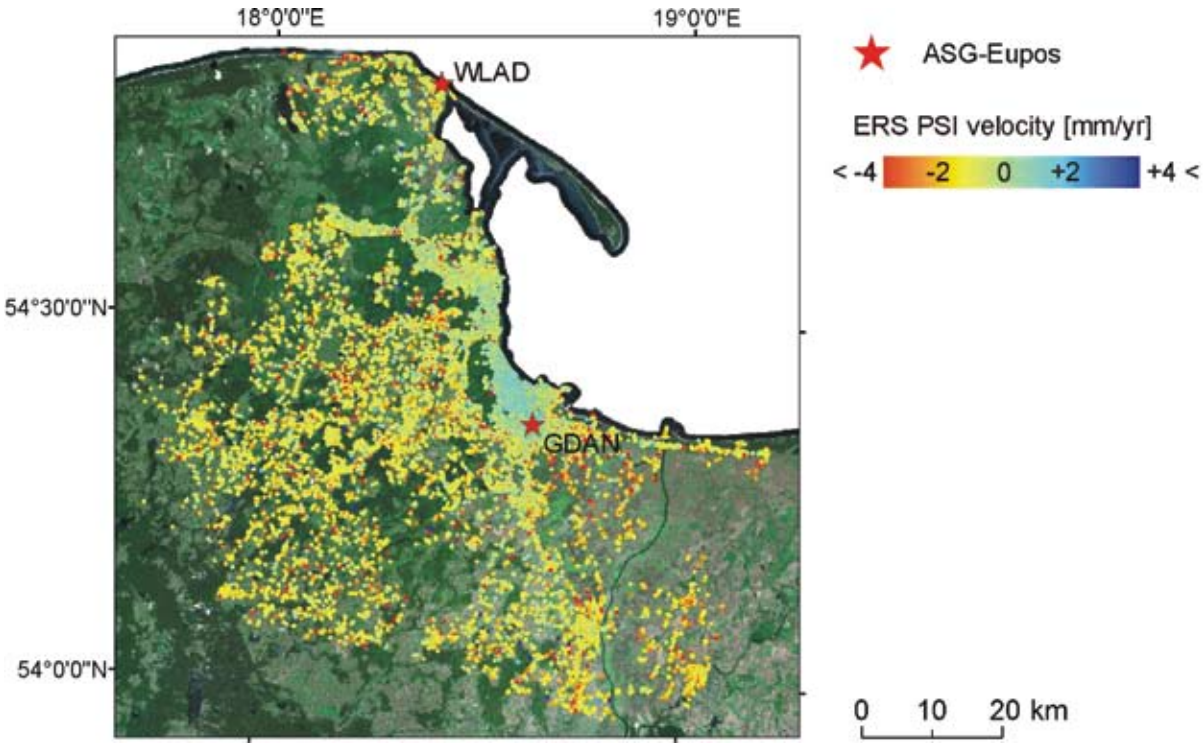

Fig. 2. General PSI results from the ERS satellite (1992–2000) and localization of two ASG-Eupos GPS permanent stations: GDAN and WLAD. Compiled by M. Graniczny, M. Przyłucka, Z. Kowalski, S. Uścinowicz and W. Jegliński, 2015

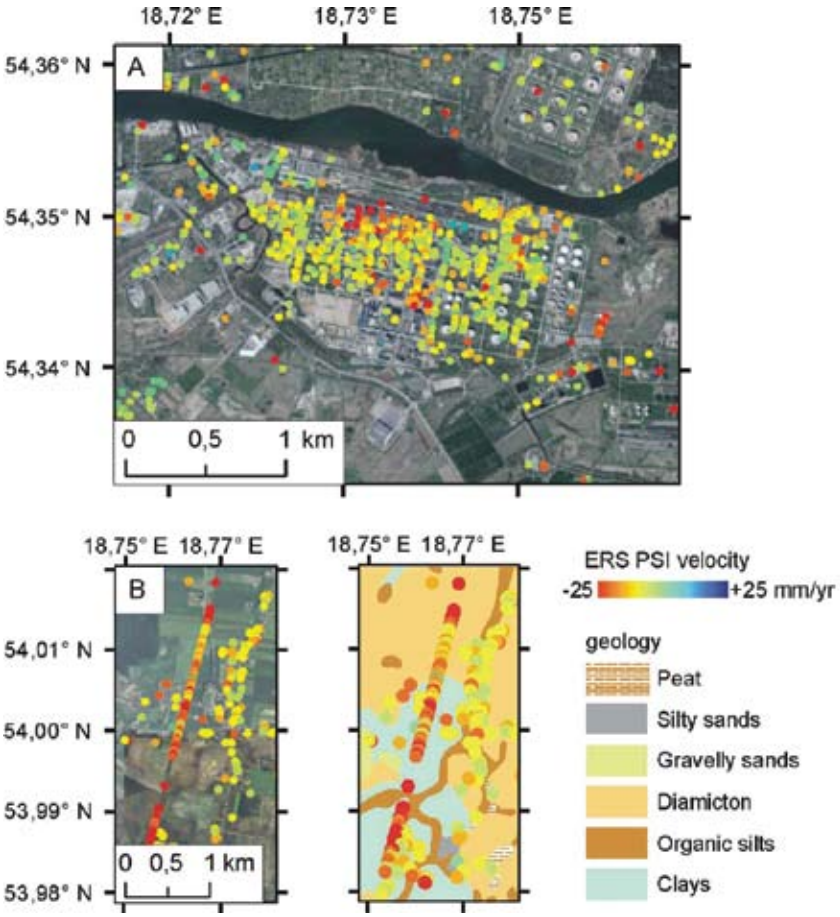

Fig. 3. Examples of local deforming areas. Green points have velocity values between –2 and +2 mm/yr; yellow between –2 and –4 mm/yr; orange and red indicate subsidence faster than –4 mm/yr. A. Rafinery Lotos Oil S. A., Gdansk. B. Railway in Subkowy. Compiled by M. Graniczny, M. Przyłucka, Z. Kowalski, S. Uścinowicz and W. Jegliński, 2015

Subkowy was detected during analyses of the PS velocities (Fig. 3B). Subsidence along the railway line seems to be due to dynamic loads caused by frequent movements of trains. Similar phenomena were observed by PSI for the railway junction of Warsaw. On the detailed geological map of Poland (SmgP) at the scale 1:50 000 (map sheets Tczew and Gniew), in section of the railway which is subsiding occur Holocene limnic muds and Late Glacial clays deposited in ice marginal lake, which are considered as 'weak sediments' susceptible for subsiding. Most probably together with dynamic loads they are responsible for the higher PS velocity values. This location should be verified during field reconnaissance, because in the future the situation may lead to real danger and damage to rails.

Comparison of measurements from piezometers with PS time series

Fig. 4A presents the area of the *Gdańsk Shipyard*. Gdańsk Shipyard was founded in 1945 as a state-owned company, on sites of the former German shipyards, *Schichau-Werft* and *Danziger Werft*, both considerably damaged in the Second World War. Over 60 years, *Stocznia Gdańsk* has delivered more than 1000 seagoing ships to owners all over the world. In recent years design and construction of ships has remained the main activity of the yard. Work for the offshore industry began in the 21st century. Gdansk shipyards have fallen on hard times. Once a place of work for over 20,000 people, the Gdansk shipyards provide only 2,200 jobs today. Therefore within the shipyard area consumption of groundwater decreased. This is clearly visible in the piezometers graphs. Consequently, as a result of aquifer hydraulic heads changes this area started to rise slightly what is confirmed by PS distribution and graphs.

The another example is coming from Wiślina village located north from Pruszcz Gdański town (Fig. 4B). This village is situated in Żuławy Wiślane (fens, plural from 'żuława') which is the alluvial delta area of Vistula, in large part reclaimed artificially by

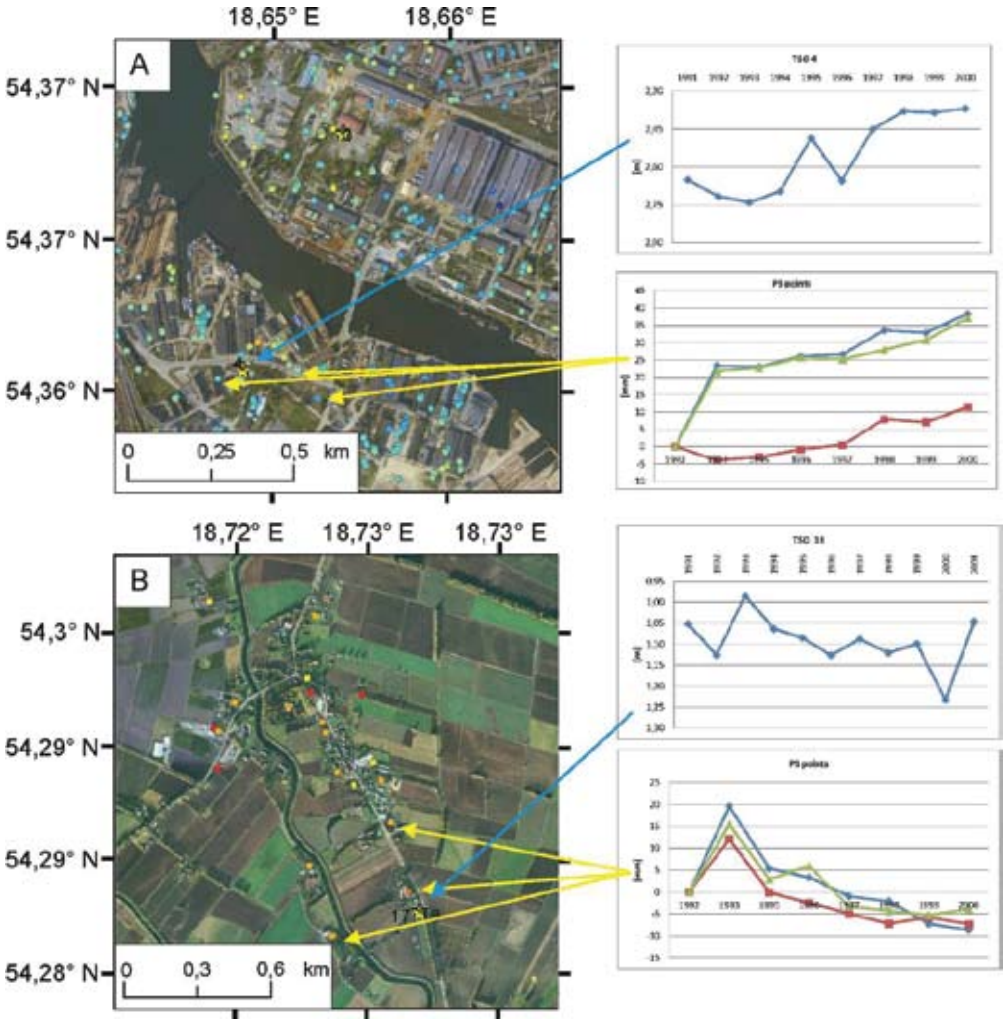

Fig. 4. Comparison of measurements from piezometers (graphs on the top in a pair) with PS points time series (graphs on the bottom in a pair). A. Gdansk shipyard. B. Wiślina village. Compiled by M. Graniczny, M. Przyłucka, Z. Kowalski, S. Uścinowicz and W. Jegliński, 2015

means of dykes, pumps, channels (over 17,000 km of total length) and extensive drainage system. In shape similar to reversed triangle formed by branching of Vistula into two separate rivers, Leniwka and Nogat at its height, confined by rivers themselves, and closed by Mierzeja Wiślana at its base. It is a deforested, agricultural plain that covers 1000 square km. This area is also characterized by shallow groundwater. As indicated at piezometers graphs groundwater level show tendency to lowering between 1991 and 2001. Most likely, it may be associated with drainage works. Consequently, the PS identified at the same period of time also show tendency to subsidence.

Dynamic-DEM

Dynamic DEM was based on PSI ERS data set which contains 78093 PS points with estimated velocity from the period 4/05/1993–7/12/2000. In Polish area of interest in SubCoast project there are two GPS reference stations – part of the ASG-EUPOS system (*http://www.asgeupos.pl*) with exact current coordinates of the stations in ITRF system and time series from the period 06.2008–11.2012 in ETRF2000 (see Fig. 2):

1. GDAN (located at Town Office of Gdansk, 3 Maja Street No.9, 80-951 Gdańsk)
2. WLAD (Space Research Centre Observatory Władysławowo, Port Marine, Hryniewickiego Street No.2, 84-120 Władysławowo, station on the harbour breakwater)

For each station the linear deformation rate in the vertical (Up) direction was estimated. Based on the GNSS time series of the GDAN station, the noise level of the GNSS measurements was detemined to be 2.7 mm (1σ). The GNSS time series and expected trends for the GDAN station are visualized in Fig. 5. Both a trend using a linear model only (red line) and a trend assuming an additional seasonal deformation behavior (green line) were estimated. The linear model results in a trend of 0.60 mm/yr. After adding the seasonal model, a trend of 0.50 mm/y was obtained, with a standard deviation of 0.06 mm/yr. The latter result was used.

The GNSS time series and estimated trends at the WLAD station are shown in Fig. 6. The time series showed a strong discontinuity in 2011. It is unclear whether this is an actual deformation signal or an artefact. Straightforward application of a linear deformation model resulted in a deformation rate of -2.80 mm/y (red line). When considering the discontinuity and assuming a seasonal behaviour, the green line is obtained with a deformation rate of 1.63 mm/y, estimated with a standard deviation of 0.10 mm/y (assuming the same noise level of the GNSS measurements of 2.7 mm).

It should be noted that the linear model of the trend of deformation rate in the vertical direction of both stations GDAN and WLAD is positive (uplift). The WLAD station is highly unreliable due to discontinuity in 2011, therefore it was decided to use only GDAN station in PSI referencing.

In case of GDAN station we used four PS on the roof of the building on which the GNSS antenna is mounted. One PS is classified as outlier and is therefore removed. The predicted PSI velocity and the offset between the GNSS and PSI velocity are indicated in Table 1. The PSI velocity is predicted by a least-squares based weighted average of the three remaining PS on the building, where the PSI standard deviations are used to describe the dispersion of the observations. Only an offset of –0.11 mm/y between the two datasets is estimated. It should be noted that the two time periods of the GNSS and PSI measurements are not overlapping. Therefore the strong assumption of a long term constant deformation rate is assumed.

In case of the WLAD station, no PS on the same object are available. For this reason, the second, surrounding area based procedure is followed. Again,

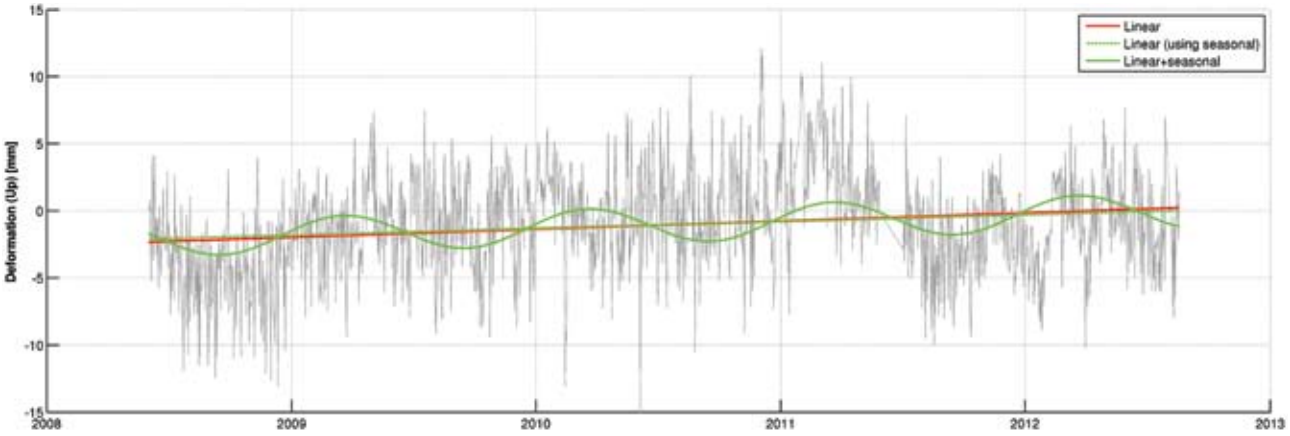

Fig. 5. GNSS time series at the GDAN station, including estimated linear trends. Compiled by F. Van Leijen and R. Hanssen, 2013

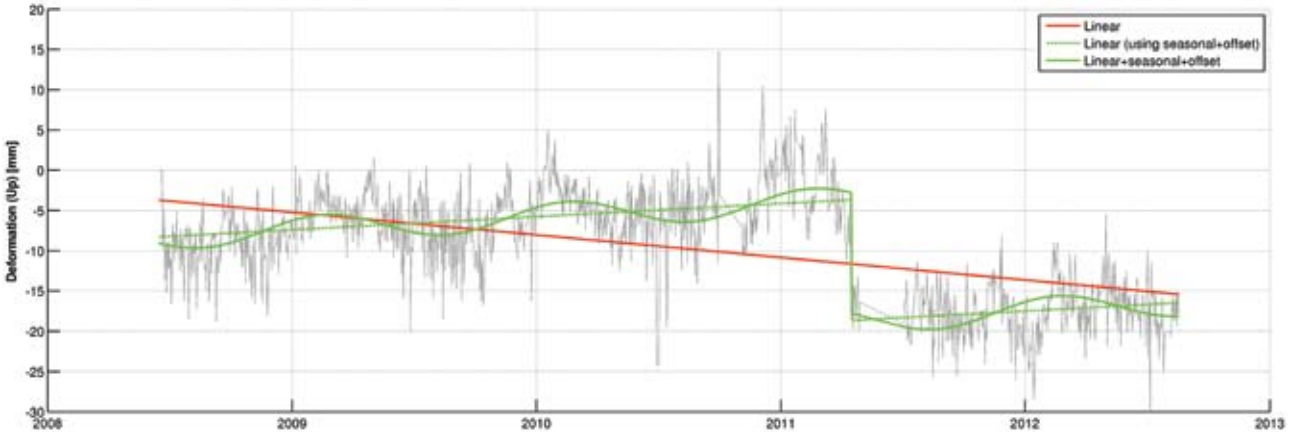

Fig. 6. GNSS time series of the WLAD station, including estimated linear trends. Compiled by F. Van Leijen and R. Hanssen, 2013

Table 1. GNSS and PSI deformation rates at the GNSS station locations, together with their standard deviations. The difference between them determines the offset

Station	GNSS velocity [mm/y]	Std GNSS velocity [mm/y]	PS velocity [mm/y]	Std PS velocity [mm/y]	Offset [mm/y]	Std Offset [mm/y]
GDAN	0.50	0.06	0.61	0.21	-0.11	0.22
WLAD	1.63	0.10	-1.55	0.13	3.18	0.16

the results are shown in Table 1. In this case, an offset of 3.18 mm/y is found. This big difference may indicate a trend in the PSI results, but, based on visual interpretation of the PSI velocities, this does not seem likely. Because of the questions regarding the integrity of the time series at the WLAD station (discontinuity in 2011), and the uncertainty in the homogeneity of the deformation field around the station, used to predict the PSI rate at the station, it is chosen to neglect the WLAD station and base the offset on GDAN station only.

Based on the estimated offset at the GDAN station of –0.11 mm/y, and the accompanying standard deviation of 0.22 mm/y, the PSI deformation rates, standard deviations (applying error propagation based on the original standard deviations and standard deviation of the offset) and time series were adapted. Hereby, the PSI data were transformed to the GNSS datum.

To prevent the influence of outliers in the PS results on the DDEM deformation model, outliers were removed based on a local filter. Hereby the velocity rate of each PS was compared to the mean velocity rate of all surrounding PS within a 2000 m radius, with a maximum of 20 PS. When the difference was larger than 2 times the standard deviation of surrounding PS velocity rates, the particular PS was classified as an outlier. This procedure is repeated for all PS. Hence, the local PS velocity field is considered, instead of a histogram cut-off based on the complete dataset.

The original dataset consisted of 78093 PS, with a deformation rate range between -26.3 mm/y and 28.0 mm/y. After outlier removal, only 71984 PS remain, with rate values between –10.7 mm/yr and 5.3 mm/yr. Hence, in total 6109 PS have been removed. To reduce the amount of data (71984 PS) a quadtree grid was created. In total 1353 quadtree blocks are obtained. The quadtree approach is based on an iterative scheme, where the variance of the PS measurements within a block determines whether or not a block is further subdivided. Hereby, a standard deviation threshold of 0.75 mm/y was applied. Furthermore, a block should at least contain 20 PS to allow further subdivision. A block is assigned a value when at least 3 PS reside within the block. The minimum and maximum allowed block sizes are 312.5 to 10 000 m, respectively.

From quadtree blokes, the grid values are obtained by Ordinary Kriging, applying a Gaussian variogram with a sill of 1.0 mm/y and a range of 14 km, in combination with a nugget of 0.5 mm/y. For each grid cell, maximum 40 quadtree blocks within a range (to the center of the block) of 42 km are used for Kriging. The result is shown in Fig. 7. The Kriging weights were used to obtain a standard deviation for each grid cell based on the standard deviations of the quadtree blocks. The final map of deformation rates shown in Fig. 7 presents rather a stable area, were movements do not exceed –3 mm per year.

One of the dominant structural elements at the studied area are two zones of lineaments interpreted at the satellite image, oriented NNW – SSE. There are: Żarnowiec and Jastrzębia Góra – Chylonia zones (Graniczny, 1994; Fig. 7). Tectonic zones following

such direction were identified also at several tectonic maps (Książkiewicz *et al*. 1974, Pożaryski, Dębowski 1984; Petelski, Sadurski 1987; Żelaźniewicz *et al*. 2011). Moreover, it is possible to see that isoamplitudes of neotectonic movement follow direction of two above mentioned lineament's zones (NNW – SSE) and changing values from –50 to +50 metres (Rühle 1961; Harff 2001; Wyrzykowski 1985). They constitute division between Łeba upland and Lower Vistula depression. There is also indication of disturbances of geological strata of Permian and Cretaceous horizons lowering to the west, along NNW – SSE zones. There is also some correlation between them and gravimetric anomalies. Taking above under consideration we can assume that these features have (neo)tectonic character.

Additional argument for existence of the low rate tectonic activity indicated comparison of tectonic zones with PS data (Deformation rates on regular grid 100 X 100 m, derived from the quadtree decomposition by Ordinary Kriging; Fig. 7). Some of the discontinuities oriented NNW – SSE and ENE – WSW create system of blocks, which separates areas characterized by different ground motion (uplift and subsidence). As mentioned before two regional NNW – SSE zones (Fig. 7, zones a and b) divide depression of Żuławy (Nowy Dwór Gdański) and coastal lowlands (between Gdańsk and Puck) from uplifted moraine areas in the west (Kościerzyna – Kartuzy – Łębork). It is also should be noted that small block determined by two direction of discontinuities (NNW – SSE and ENE – WSW; Fig. 7, zones a and c) located in the northern coastal zone between Łeba and Żarnowiec shows clear tendency for uplifting and differs substantially from neighbouring areas (blocks). Taking above under consideration we can assume that these above mentioned discontinuities are tectonically active.

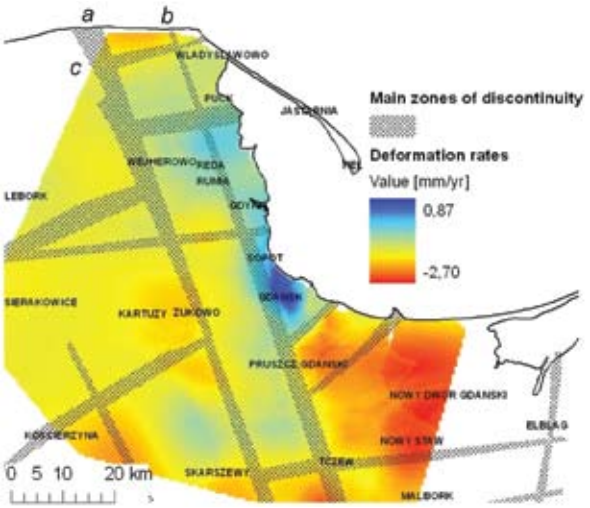

Fig. 7. Distribution of the deformation rates on regular grid (100 x 100 m), derived from the quadtree decomposition by Ordinary Kriging versus main zones of discontinuities. Tectonic zones (after Graniczny, 1994): a – Żarnowiec; b – Jastrzębia Góra-Chylonia; c – Białogóra-Władysławowo. Compiled by M. Graniczny, M. Przyłucka, Z. Kowalski, S. Uścinowicz and W. Jegliński, 2015

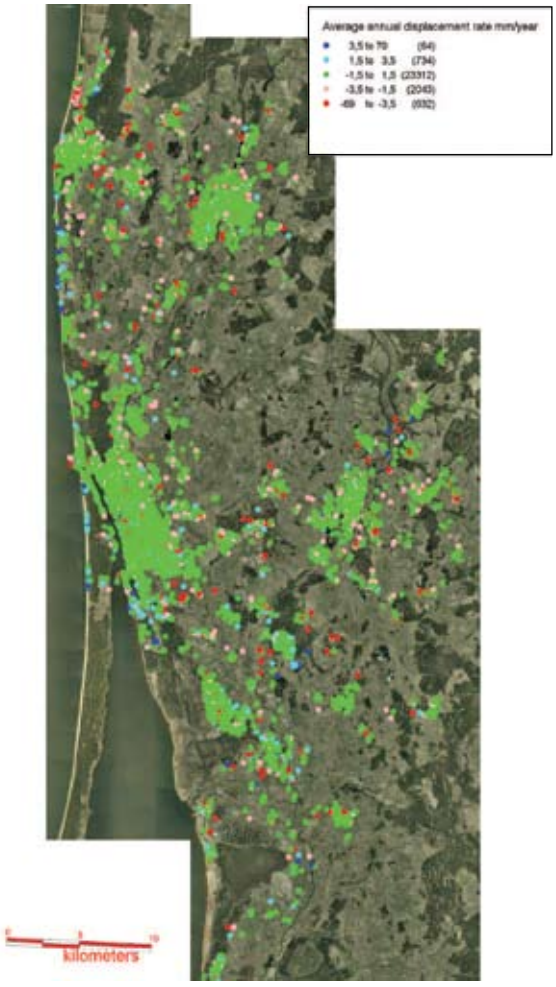

Fig. 8. Scatter plot of average terrain-motion for 26,785 points generated by satellite-based Persistent Scatterer Interferometry (PSI) for the Lithuanian Baltic Sea coastal area. Compiled by V. Minkevičius, 2015

RESULTS AND INTERPRETATION – LITHUANIAN CASE STUDY

Persistent Scatterer general results

The main validation activity was the observation of in-situ PSI points. For motion interpretation purposes, the PSI dataset was combined with a digital orthophoto based on aerial photos and the Digital Elevation Model (DEM) for the Lithuanian Baltic Sea coast prepared from the Shuttle Radar Topography Mission (SRTM) data products and LIDAR also. This enables precise location of positive and negative PS velocities, indicative of upward and downward displacements respectively. The PSI dataset was divided into five categories (Fig. 8):

- PS with velocities greater than +3.5 mm/yr

- PS between +3.5 mm/yr and +1.5 mm/yr
- PS between +1.5 mm/yr and -1.5 mm/yr
- PS between -1.5 mm/yr and -3.5 mm/yr
- PS with velocities lower than –3.5 mm/yr

The PSI dataset of the Lithuanian Baltic Sea coastal area has been analysed with the aid of different thematic and geological mapping data. The PSI results suggest that in the studied area there has been no severe coastal deformation occurring between 1992–2000.

The possible (neo)tectonic activity can be detected along or near known tectonic faults. The PSI dataset of AOI is characterized by the irregular distribution of moving and stable PS. The location of tectonic faults and available PSI points data doesn't show evidence for the active (neo)tectonic movements (Fig. 8, 9) in the AOI . There is no visible spatial or linear trend of PS, which could provide some evidence of a possible relation between ground motions and tectonic or neotectonic activity of the studied area (Fig. 9).

However, performed activities also suffered of intrinsic problems due to low density of PS points in studied area. The limitation of SAR PSI points has been related to the vegetation and seasonal weather conditions such as snow cover. This causes lack of reflecting surfaces. Also some doubts concern with suitability to use the received SAR data for understanding the (neo)tectonic activity of the area due to

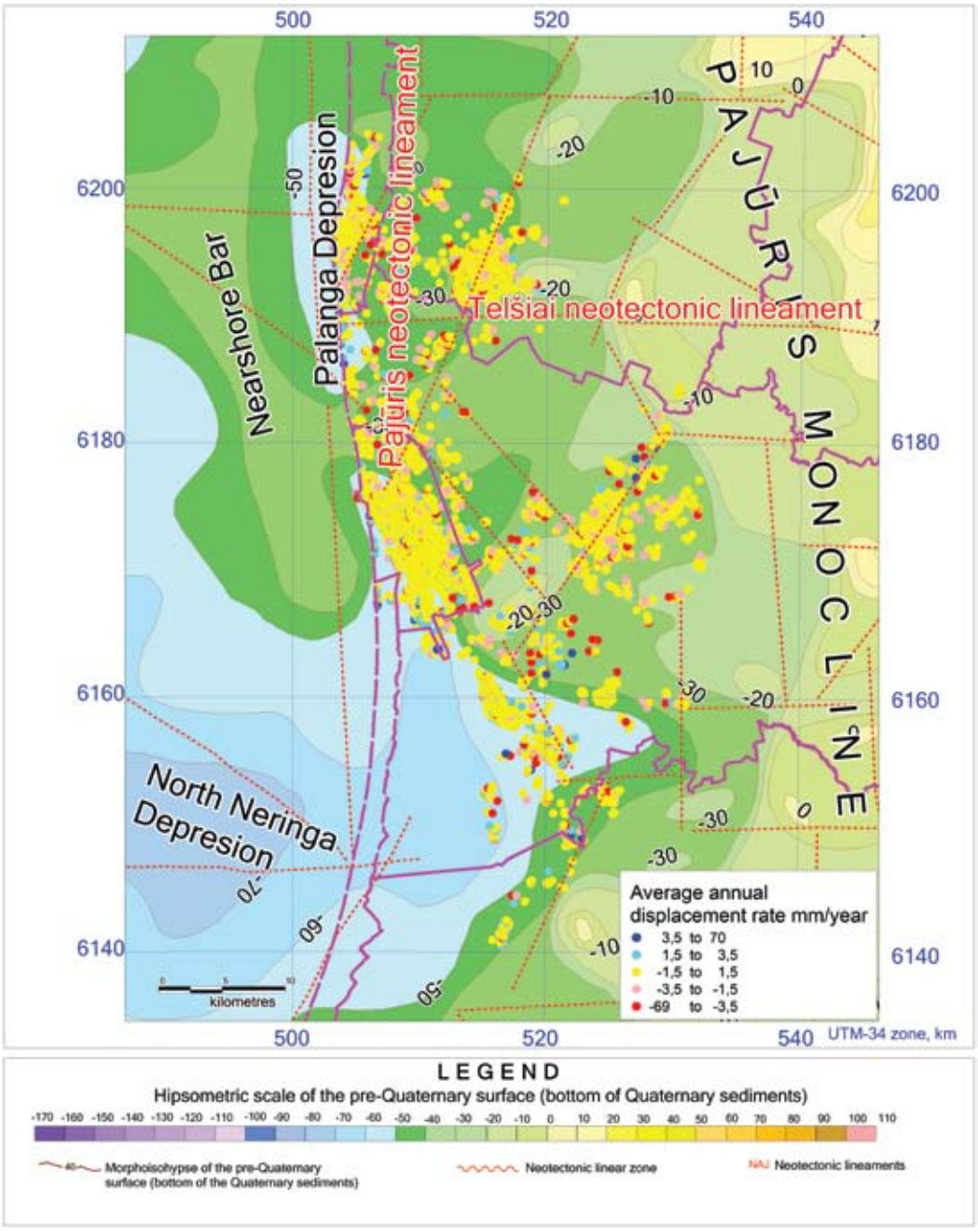

Fig. 9. Neotectonic map (after A. Šliaupa, 2005) and PSI points. Compiled by V. Minkevičius, 2015

limited time scale of available PSI data. In general the (neo)tectonic movements could have a low rates in the studied area, therefore the larger time scale information could improve confidents in the results. To understand the (neo)tectonic processes, their rate and influence on Quaternary sediments, (neo)tectonic structures and movements, further complex of studies and services should be used. The basic studies of the sub-Quaternary relief, Quaternary succession, modern relief and drainage system and their comparison with DInSAR data from different satellites, the GPS campaigns and traditional geodetic levelling data could help properly understand the recent tectonic activity of a region, and to assess the associated hazards.

The review of the PS dataset has enabled identification of several sites within the coastal area characterized by spatially consistent concentrations of negative PS (Fig. 8). These localities were checked during the field reconnaissance. The examples of movements detected by PSI examined in the studied area included subsidence linked to location and deformation of engineering constructions (e.g. deformations in the embankments of Klaipėda Sea Port, deformation of the security installations of the Palanga – Klaipėda road), compaction of organic or weak soils, eolian accumulation or deflation processes of the sand dunes. The particular sites of negative movements and their interpretation are presented below.

There is no obvious evidence of neotectonic movements in relation to local sea level rise as well as the regional scale subsidences, however a few local subsidences have been observed in Klaipėda Sea Port area. PSI data show good correlation with deformations in the embankment of Klaipėda Sea Port (Fig. 10). The analysis of the PS spatial distribution within the context of the lithologic boundaries of the geological map indicated some interesting relationships.

The analysis of the PS spatial distribution within the context of the lithologic boundaries of the geological map indicated some interesting interrelations. One example comes from the Vanagai area (Lithuania), where the coincidence between the genesis of the different sediments and negative velocity PS is observed (Fig. 11). Despite the fact that the sediments of the same geotechnical strengths are present, the differences in genesis influence different behaviour of soil compaction.

The processes of the eolian accumulation and formation of new layers of dunes has been detected in Palanga area (Figs 12 and 13) and show good correspondence with PS data.

Dynamic-DEM

Dynamic DEM for Lithuanian coast was created using DEM (Digital Elevation Model), PSI data (points and

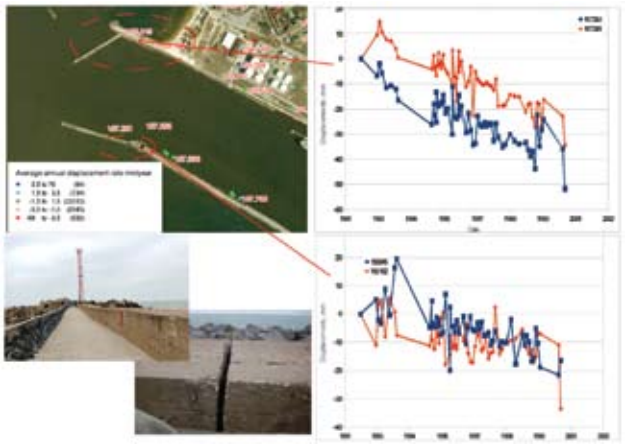

Fig. 10. Deformations of the embankment in the Klaipėda Sea Port. Compiled by V. Minkevičius and V. Mikulėnas, 2015

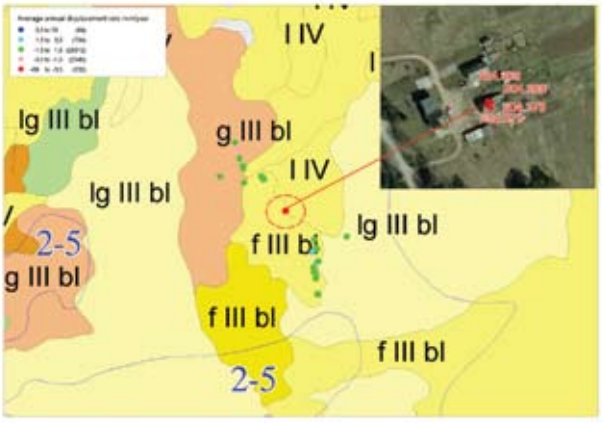

Fig. 11. PSI data results vs. genesis of the different sediments (f III bl – fluvioglacial deposits of Baltija Stage; l IV – lacustrine sediments of Holocene; lg III bl – glaciolacustrine sediments of Baltija Stage; g III bl – glacial deposits of Baltija Stage; colours indicate strength of soils: yellow (from light to dark) – coarse soils from loose to dense; brown (from like to dark) – find soils from weak to hard; green – mixed soils). Compiled by V. Minkevičius, 2015

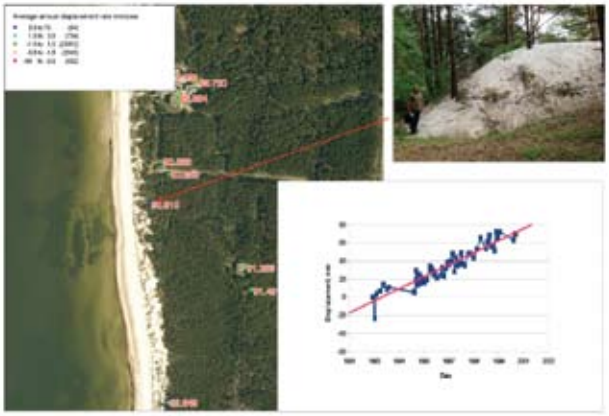

Fig. 12. Eolian accumulation in the Palanga area and formation of new layers of the dune shows clear correlation with PS data. Compiled by V. Minkevičius and V. Mikulėnas, 2015

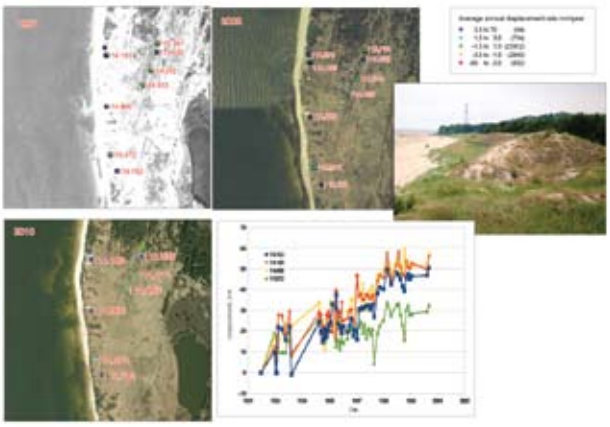

Fig. 13. Eolian accumulation in the Šaipiai area and correlation with PS data. Compiled by V. Minkevičius and V. Mikulėnas, 2015

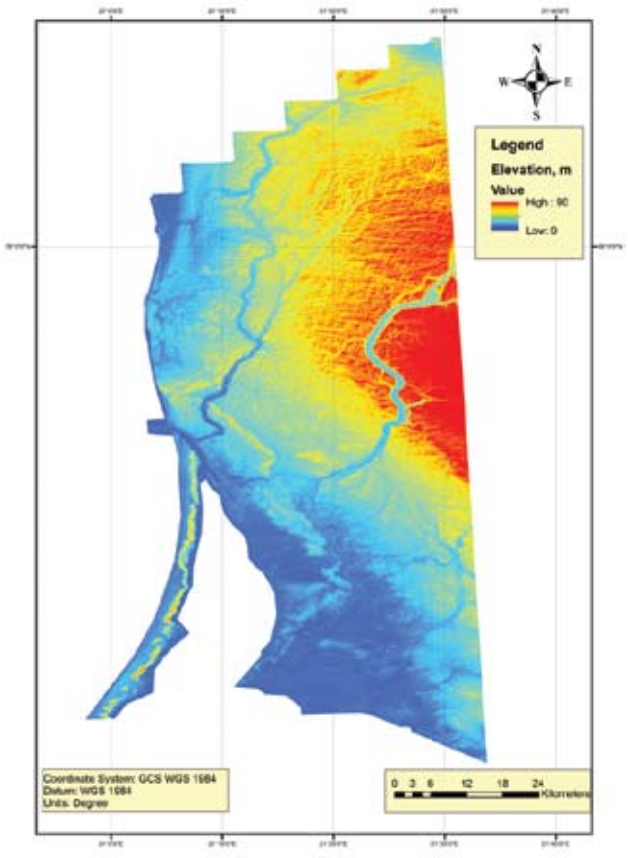

Fig. 14. Digital Elevation Model from LIDAR data (raw data © Nacionalinė žemės tarnyba) for the Lithuanian coastal area. Compiled by V. Minkevičius, 2015

velocities). The PSI was corrected with GPS measurements. DEM was created from LIDAR data. LIDAR data was filtered and pre-processed. Only surface elevations were used. The density of the LIDAR was 3–4 points per sq. meter. Vertical standard deviation is 30 cm, horizontal 60 cm. The initial projection of the data is LKS-94 (Lithuanian coordinate system).

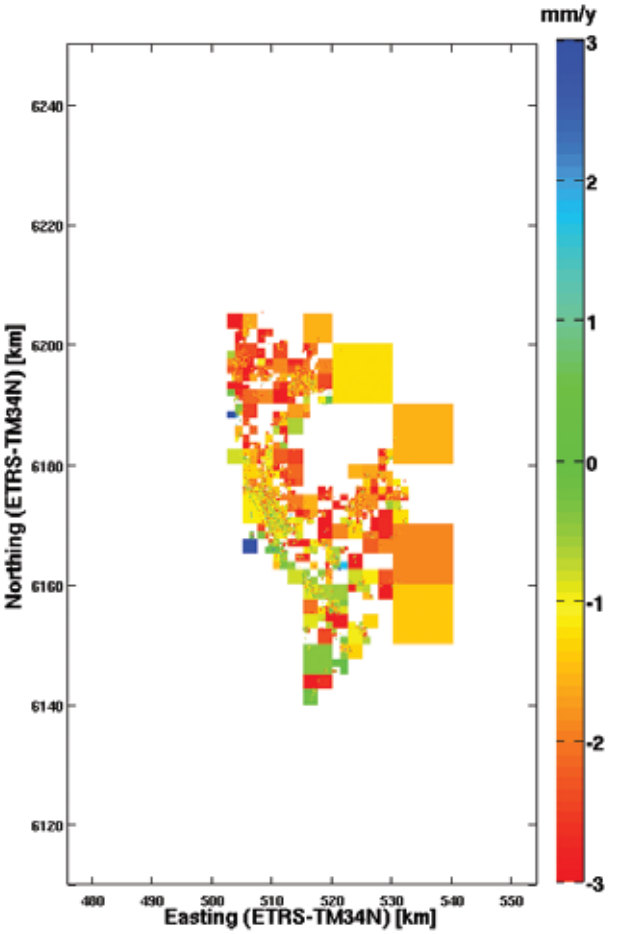

Fig. 15. Quadtree of deformation velocity rates [mm/y]. The original PS are visualized as well. Compiled by F. Van Leijen and R. Hanssen, 2013

Height system is Baltic height system. The cell size of the grid is 5x5 m. After generation of the grid it was re-projected to WGS-84 coordinate system (Fig. 14).

Fugro NPA Ltd. prepared a dataset of PSI points. Velocity values were transformed from VEL_{los} values to $VEL_{vertical}$ values for Dynamic DEM generation. The reference point of PS has also been changed. It was chosen based on GPS measurements. The reference point movement according to GPS measurements is 1.88 +/–0.31 mm/yr. To reduce the amount of data (24723 PS) a quadtree grid is created. In total 1066 quadtree blocks are obtained. The quadtree approach is based on an iterative scheme, where the variance of the PS measurements within a block determines whether or not a block is further subdivided. Hereby, a standard deviation threshold of 0.75 mm/y is applied. Furthermore, a block should at least contain 20 PS to allow further subdivision. A block is assigned a value when at least 3 PS reside within the block. The minimum and maximum allowed block sizes are 312.5 to 10 000 m, respectively (Fig. 15).

From quadtree blokes, the grid values are obtained by Ordinary Kriging, applying a Gaussian variogram

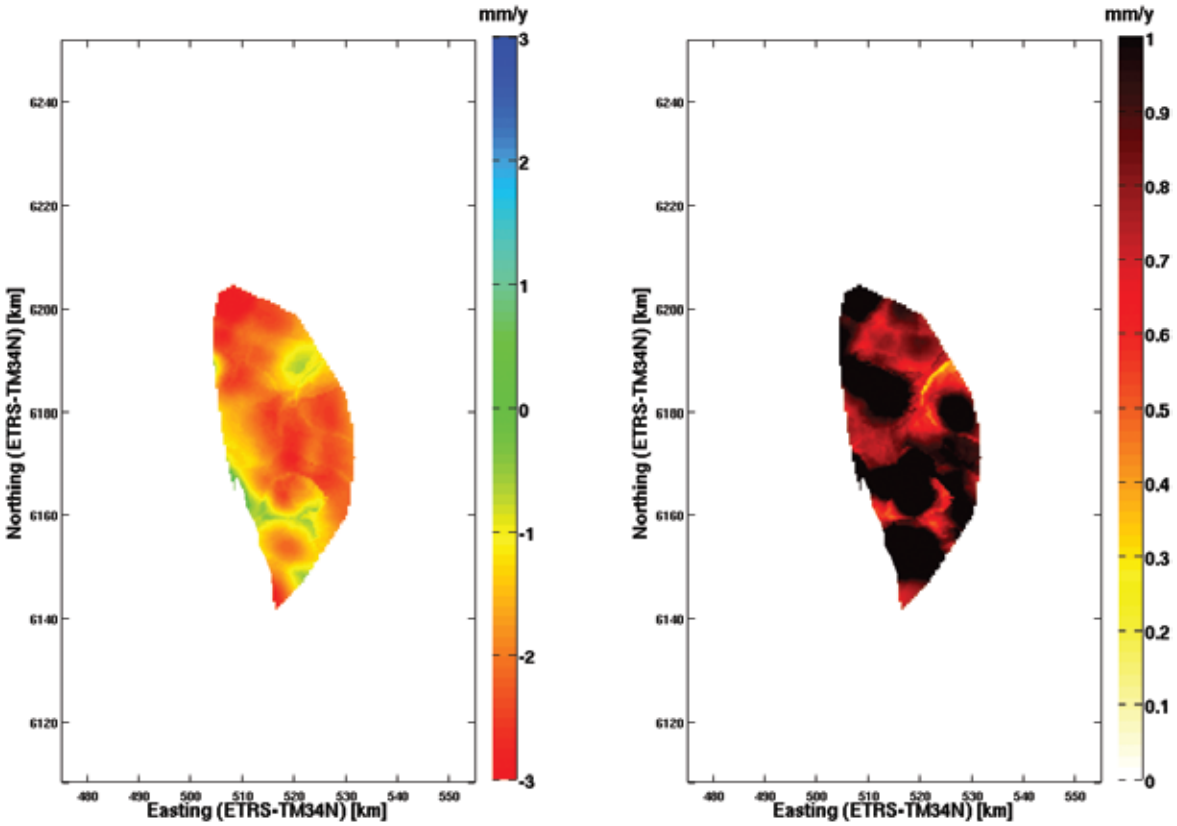

Fig. 16. Left: deformation rates on regular grid (100 x 100 m), derived from the quadtree decomposition by Ordinary Kriging. Right: associated standard deviations of the grid cells. Compiled by F. Van Leijen and R. Hanssen, 2013

with a sill of 1.0 mm/y and a range of 7 km, in combination with a nugget of 0.5 mm/y. For each grid cell, maximum 40 quadtree blocks within a range (to the center of the block) of 42 km are used for Kriging. Only grid cells within the convex hull of the PSI measurement points are assigned a value. The Kriging weights are used to obtain a standard deviation for each grid cell based on the standard deviations of the quadtree blocks (Fig. 16). The model of deformation rates can be used to predict possible surface changes which can be used for flood risk analysis.

CONCLUSIONS

Along the Polish and Lithuanian Baltic Coast there is no clear wide-scale deformation visible, most of the detected PS points are stable. These vertical movements, which were estimated by PSInSAR in the period 1992–2000, do not constitute a real geohazard to the area. A dozen designated areas with high concentration of PS points with deformation rates<–2 mm/y may have different reasons for these movements: subsidence of buildings, the ground water level decrease. Field reconnaissance in these areas should be planned.

The new innovative product – Dynamic DEM (DDEM) was demonstrated. The deformation model defined by the Subcoast project normally needs to be created by merging InSAR, satellite navigation (GNSS), optical leveling and/or gravimetry measurements. Elaboration of DDEM enables more effective comparison between PS and tectonic features.

The comparison of PS data (Deformation rates on regular grid 100 X 100 m, derived from the quadtree decomposition by Ordinary Kriging) with tectonic zones indicated additional argument for existence of the low rate tectonic activity. Majority of the discontinuities oriented NNW – SSE and ENE – WSW create system of blocks, which separates areas characterized by different ground motion (uplift and subsidence).

Comparison of PS time series with groundwater changes shows a direct correlation, confirming impact of groundwater on subsidence or uplift of the ground surface. The results of the geological interpretation demonstrated that the examples of movements detected by PSI include subsidence linked to deformation of engineering constructions, compaction of organic or weak soils, and eolian accumulation or deflation processes of the sand dunes.

ACKNOWLEDGMENTS

The authors would like to thank Prof. Victor V. Klemas (University of Delaware), Prof. Albertas Bitinas (Klaipėda University) and Dr. Gerardo Herrera

Garcia (Geological Survey of Spain, Madrid) for the thorough review and very helpful comments, which allowed significantly improve our manuscript. The research was done under the SubCoast project, which is a collaborative project under THEME FP7-SPACE-2009-1 of the Seventh Framework Programme of the European Commission (GA No. 242332).

REFERENCES

Bernardino, P., Fornaro, G., Lanari, R., Sansosti, E., 2002. A new algorithm for surface deformation monitoring based on small baseline differential SAR interferograms. *IEEE Transactions on Geoscience and Remote Sensing 40 (11)*, 2375–2383. http://doi.org/10.1109/TGRS.2002.803792

Bitinas, A., Repečka, M., Kalnina, L., 1999. Correlation of tills from the South–Eastern Baltic bottom and nearshore boreholes. *Baltica Special Publication 12,* 5–10.

Bitinas, A., Damušytė. A., Hütt, G., Jaek, I., Kabailienė, M., 2001a. Application of the OSL dating for stratigraphic correlation of Late Weichselian and Holocene sediments in the Lithuanian Maritime Region. *Quaternary Science Reviews 20*, 767–772.

Bitinas A., Damušytė., A., Hütt, G., Martma, T., Ruplėnaitė, G., Stančikaitė, M., Ūsaitytė, D., Vaikamäe, R., 2001 b. Stratigraphic correlation of Late Weichselian and Holocenedeposits in the Lithuanian Coastal Region. *Proceedings of the Estonian Academy of Sciences, Geology 49 (3),* 200–217.

Bitinas, A., Žaromskis, R., Gulbinskas, S., Damušytė, A., Žilinskas, G., Jarmalavičius, D., 2005. The results of integrated investigations of the Lithuanian coast of the Baltic Sea: geology, geomorphology, dynamics and human impact. *Geological Quarterly 49 (4)*, 355–362

Bovenga, F., Nutricato, R., Recife, A., Wasowski, J., 2006. Application of multi-temporal differential interferometry to slope instability detection in urban/peri-urban areas. *Engineering Geology 88 (3-4)*, 218–239. http://doi.org/10.1016/j.enggeo.2006.09.015

Colesanti, C., Wasowski, J., 2006. Investigating landslides with satellite Synthetic Aperture Radar (SAR) interferometry. *Engineering Geology 88 (3-4)*, 173–199. http://doi.org/10.1016/j.enggeo.2006.09.013

Colesanti, C., Ferretti, A., Prati, C., Rocca, F., 2003. Monitoring landslides and tectonic motions with the Permanent Scatterers Technique. *Engineering Geology, Special Issue on Remote Sensing and Monitoring of Landslides 68 (1)*, 3–14.

Culshaw, M., 2009. Stoke-on-Trent, United Kingdom. *In* R. Capes and S. Marsh (eds), *The Terrafirma Atlas—The Terrain-motion Information Service for Europe,* GMES–ESA, June 2009, TerraFirma project, ESA publication, p. 43.

Del Ventisette, C., Ciampalini, A., Manunta, M., Calò, F., Paglia, L., Ardizzone, F., Mondini, A.C., Reichenbach, P., Mateos, R.M., Bianchini, S., Garcia, I., Füsi, B., Deák, Z.V., Rádi, K., Graniczny, M., Kowalski, Z., Piatkowska, A., Przyłucka, M., Retzo, H., Strozzi, T., Colombo, D., Mora, O., Sánchez, F., Herrera, G., Moretti, S., Casagli, N., Guzzetti, F., 2013. Exploitation of large archives of ERS and ENVISAT C-band SAR data to characterize ground deformations. *Remote Sensing 5 (8)*, 3896–3917.

Ferretti, A., Prati, C., Rocca, F., 2001. Permanent Scatterers in SAR Interferometry. *IEEE Transactions on Geoscience And Remote Sensing 39 (1)*, 8–20. http://doi.org/10.1109/36.898661

Ferretti, A., Prati, C., Rocca, F., Wasowski, J., 2006. Satellite interferometry for monitoring ground deformations in the urban environment. *Proceedings 10th IAEG Congress*, Nottingham, UK (CD-ROM).

Gabriel, A.K., Goldstein, R.M., Zebker, H.A., 1989. Mapping small elevation changes over large areas: differential radar interferometry. *Journal of Geophysical Research 94*, N°B7, 9183–9191. http://doi.org/10.1029/JB094iB07p09183

Graniczny, M., 1994. Tectonic discontinuities in view of correllation of the multi-thematic geological data on examples from Żarnowiec and Kłodzko area. *Instrukcje i Metody Badań Geologicznych*, Zeszyt *54*, 1–82. [In Polish].

Graniczny, M., 2009. Sosnowiec, Poland. *In* R. Capes and S. Marsh (eds), *The Terrafirma Atlas—The Terrain-motion Information Service for Europe,* GMES–ESA, June 2009, TerraFirma project, ESA publication, p. 34.

Harff, J., 2001. Recent vertical movements of the Earth crust, geological perspective of global climate change. *AAPG Studies in Geology*, 231–246.

Hay-Man, Mg A., Chang, H.C., Ge, L., Rizos, C., Omura, M., 2009. Assessment of radar interferometry performance for ground subsidence monitoring due to underground mining. *Earth, Planets and Space 61 (6),* 733–745.

Książkiewicz, M., Oberc, J., Pożaryski, W., 1974. Tectonic Map of Poland 1:1 500 000, Instytut Geologiczny, Warszawa.

Massonnet, D., Feigl, K., 1998. Radar interferometry and its application to changes in the Earth's surface. *Reviews of Geophysics 36*, 441–500. http://doi.org/10.1029/97RG03139

Mojski, E., 1988. Development of the Vistula River Delta and evolution of the Baltic Sea, an attempt to chronological correlation. *Geological Survey of Finland, Special Papers 6*, 39–51.

Petelski, K., Sadurski, A., 1987. Genesis of the Reda-Łebaice marginal valley in view of the mass transport and heat theory. *Czasopismo geograficzne LVIII*, 450–456. [In Polish].

Pikies, R., 2000. Quaternary substratum in the Kaszuby Pomerania region. *Proceedings of VIIth Conference on 'Stratigraphy of Polish Pleistocene'*, Polish Geological Institute, 65–69. [In Polish].

Pokorski, J., Modliński, Z., 2007. Geological Map of the western and central part of the Baltic depression with-

out Permian and younger formations, 1:750 000. Polish Geological Institute, Warszawa.

Pożaryski, W., Dembowski, Z., 1984. Geological Map of Poland and adjoining countries, 1: 1 000 000, Geological Institute, Warszawa.

Rühle, E., 1961. *Quaternary substratum and its imapct for distribution and character of quaternary sediments in Poland.* Geological Institute, Warszawa.

Šliaupa, A., 2005. Neotectonic map of Lithuania and adjacent areas, 1:1 000 000. *Evolution of Geological Environment in Lithuania*, Vilnius, 2005, CD ROM.

Tomás, R., Romero, R., Mulas, J., Marturià, J. J., Mallorquí, J. J., López-Sánchez, J. M., Herrera, G., Gutierrez, F., Gonzalez, P. J., Fernandez, J., Duque, S., Concha-Dimas, A., Cocksley, G., Castaneda, C., Carrasco, D., Blanco, P., 2014. Radar interferometry techniques for the study of ground subsidence phenomena: a review of practical issues through cases in Spain. *Environmental Earth Sciences 71 (1)*, 163–181.

Uścinowicz, S., Zachowicz, J., Graniczny, M., Dobracki, R., 2004. Geological structure of the Southern Baltic coast and related hazards. *Polish Geological Institute Special Papers 15*, 61–67.

Wasowski, J., Recife, A., Bovenga, F., Nutricato, R., Gostelow, P., 2002. On the applicability of SAR interferometry techniques to the detection of slope deformations. *Proceedings 9th IAEG Congress, Durban,* South Africa, 16–20 Sept. 2002, CD ROM.

Werner, C., Wegmüller, U., Strozzi, T., Wiesmann, A., 2003. Interferometric point target analysis for deformation mapping. Proceedings, *IEEE International Geoscience Remote Sensing Symposium (IGARSS 2003), Vol. 7,* 4362–4364. http://doi.org/10.1109/igarss.2003.1295516

Wyrzykowski, T., 1985. Map of the contemporary vertical velocities of the Earth's crust at the Polish territory at a scale 1: 2 500 000. *Institute of Geodesy and Cartography*, Warszawa. [In Polish].

Żelaźniewicz, A., Aleksandrowski, P., Buła, Z., Karnkowski, P. H., Konon, A., Oszczypko, N., Ślączka, A., Żaba, J., Żytko K., 2011. Tectonic regionalization of Poland. *Committee of Geological Sciences, Polish Academy of Sciences*, Wrocław, 1–60. [In Polish].